Fluorescence study of tetracaine–cyclodextrin inclusion complexes

Iván Iglesias-García[a], Isabel Brandariz[a] & Emilia Iglesias[a*]

[a] Departamento de Química Física e E. Q. I. Facultad de Ciencias , Universidad de La Coruña , La Corunña,Spain

Supramolecular Chemistry, Volume 22, Issue 4, 2010, pages 228-236

Received: 23 Apr 2009, Accepted: 31 Aug 2009, Published online: 17 Feb 2010

DOI: 10.1080/10610270903304400

To cite this article: Iván Iglesias-García , Isabel Brandariz & Emilia Iglesias (2010) Fluorescence study of tetracaine–cyclodextrin inclusion complexes, Supramolecular Chemistry, 22:4, 228-236, DOI: 10.1080/10610270903304400

Abstract

The steady-state fluorescence emission from the local anaesthetic tetracaine (TCA) in water–solvent mixtures and in the presence of α-, β- and γ-cyclodextrin (CD) was investigated at various pH values. Emission was observed from the locally and the intramolecular charge transfer excited states. The TCA–CD system was found to be characterised by 1:1 associate in every case. The association constants of each complex were determined.

Keywords

cyclodextrins, tetracaine, fluorescence, stability constants

Introduction

It is generally believed that interaction of the anaesthetic molecules with membrane lipids or membrane proteins leads to the inactivation of neuronal ion channel activity (*1*). Tetracaine [TCA, 2-dimethylamino-ethyl-4(*N*-butylamine) benzoate] is one of the most widely studied tertiary amine local anaesthetics (*2* , *3*). The absorption and the ability of this drug to cross biological membranes are pH-dependent, since TCA can exist in neutral, singly or doubly positively charged form. The use of natural cyclodextrins (CDs) as drug carriers provides the solution to many difficulties in drug formulation that includes poor bioavailability, limited shelf life or restricted utility when the drug is irritating to skin, membranes, tissues and so on.

Natural CDs are water-soluble cyclic oligosaccharides that behave in aqueous solutions as pre-organised hosts that form hydrophobic cavities with hydrophilic external walls (*4* , *5*). The formation of inclusion complex means that compatibility is reached between the host and the guest in terms of the polarity and stereochemistry; in this process, the guest molecule experiences a non-polar environment and possesses a decreased freedom for bulk and intramolecular rotations, in the rigid non-polar CD cavity. This ability of CDs to accommodate guest molecules of appropriate size in their cavities has been utilised to control photophysical and photochemical properties (*6* , *7*) or chemical reactivity (*8* , *9*) of molecules. The restricted shape and size and the hydrophobic nature of the cavities of CDs offer the opportunity to carry out selective phototransformations and to investigate specific aspects of photochemical mechanisms. In addition, in chromophoric species that can be entirely enclosed into de CD cavity, direct protection from quencher can take place as long as the probe remains inside the cavity. The analysis of the changes in physical and chemical properties of the complexed guest provides information about the structure of the complex, the stoichiometry and stability.

The intramolecular charge transfer (ICT) phenomenon, first introduced by Grabowski et al. (*10*) to explain the dual fluorescence emission observed by Lippert et al. (*11*) in 4-(dimethyl)amino benzonitrile (DMABN), is strongly dependent on the medium polarity and viscosity and has been the subject of several studies from the early 1970s (*12-24*). On the basis of the fluorescence features, such as maxima of emission bands, fluorescence lifetimes and relative intensities of the short wavelength (SW) due to locally excited (LE) state and long wavelength (LW) due to the ICT emissions of DMABN complexes, different geometries were proposed for the inclusion in the α- or β-CD cavities.

Recently, the study of fluorescence emission and chemical reactivity of novocaine (2-diethylamino-ethyl,4-aminobenzoate) has been carried out in aqueous β-CD solutions (*25*). In the present study, we report on the influence of complexation with α-, β- and γ-CD on the

TCA excited state properties. The obtained results provide information on the effect of environment on LE and ICT emissions and on the stability and geometry of the inclusion complexes.

Experimental

High-purity TCA·HCl and CDs were purchased from Sigma-Aldrich (St Louis, MO, USA). Dioxane, dimethylsulphoxide (DMSO), methanol (MeOH) and acetonitrile (AN) (uvasol grade) were from Merck. Twice distilled water obtained under potassium permanganate solution was used for preparing solutions and buffers.

Concentrated stock solution of the hydrochloric anaesthetic salt was prepared in water and frequently renewed. The concentration of TCA was determined by weighing the appropriate quantity of the salt and the consequent dilution of the stock solution.

Potentiometric measurements were carried out in a jacket cell that was kept at constant temperature (25°C) by circulating water from a thermostat. Purified nitrogen was bubbled through the solutions to ensure thorough homogenisation and CO_2 removal. A Crison microBu 2030 automatic burette furnished with a 2.5 ml syringe for dispensing the titrant was used. The burette was controlled via a computer that was used to read the emf values from a Crison micropH 2000 pH meter, connected to two electrodes: a glass electrode radiometer pHG211 and a reference electrode radiometer REF201.

Absorption spectra were recorded on a Uvikon-Kontron 942 double beam spectrophotometer fitted with thermostated cell holders at 25°C. The concentration of TCA was about 6.5×10^{-5} M. Data acquisition and analysis of UV–vis spectra were performed with a software supported by the manufacturer and converted to ASCII format for their analysis with common packet programs.

Steady-state fluorescence spectra were recorded on an SLM Aminco-Bowman series 2 spectrofluorimeter fitted with a 150W Xenon lamp at 25°C. Data acquisition and analysis of fluorescence spectra were performed with the Fluorescence Data Manager Software supported by Aminco. Excitation and emission slits were fixed at 4 and 2 nm, respectively, the excitation wavelength was set at 300 nm and the emission intensity of fluorescence was recorded at 346 nm. In all measurements, the emission spectra, collected from 315 to 400 nm, were obtained from solutions of a constant TCA concentration of ~9 μM, chosen in a way such that the absorbance of the sample at 300 nm (the excitation wavelength) was lower than 0.2 absorbance units, and variable CD concentration.

Results

TCA is a tertiary amine that also contains a secondary amine group bonded to the phenyl ring (Scheme 1).

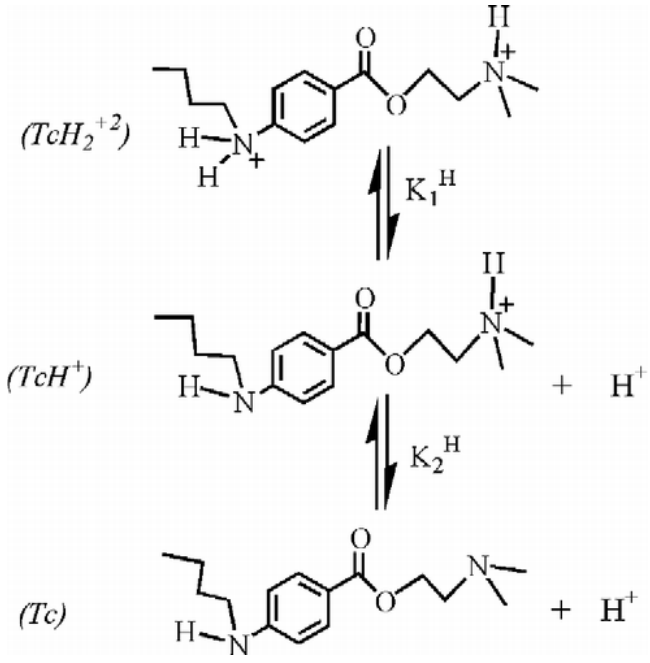

Scheme 1 Acid–base ionisation equilibrium of TCA in water.

The absorption spectrum of TCA (62 μM) in water at 25°C is characterised by two structureless bands with λ_{max} = 226 and 309 nm. Both the longer (LW, assigned to the $S_0 \rightarrow S_1$ transition) and shorter (SW, assigned to the $S_1 \rightarrow S_2$ transition) wavelength bands exhibit a slight blue shift in low dielectric media (Table 1). In strong aqueous acid media (pH < 2), the LW absorption markedly decreases, whereas, in mild acid (or neutral) aqueous media, the maximum was observed at 310 nm, but shifts to 306 nm in alkaline medium. The pK_a values of tertiary and secondary amine groups of TCA are largely different. The corresponding values have been determined by potentiometry using NaCl of 0.10 M ionic strength. The results are reported in Table 2 along with the values determined from the spectroscopic titration method (*26*) and literature data (*27*). Therefore, three different absorbing species of TCA can be considered on varying the pH of the medium, which correspond to TcH_2^{+2}, $TcH^+$and Tc (Scheme 1). At very low pH, the strongest absorption was observed at 228 nm (SW, due to π → π* transition), whereas either mild acid or alkaline medium favours the low energetic *n* → π* transition (the auxochrome secondary amine group is deprotonated) and a strong absorption at 310/306 nm (LW) was, respectively,

observed for the acid and alkaline medium. A progressive blue shift of LW and SW bands on increasing pH was observed.

Table 1 Solvent properties, values of the ratio of fluorescence emission intensities of LE to ICT states and UV–vis absorption data.

Solvent	ϵ_r [a]	μ (D)[b]	I_{LE}/I_{ICT} [c]	λ_{max} (log ε)[d]
Dioxane	2.2	0.45	2.28	224(4.0); 310(4.5)
DMSO	46.45	4.05	1.77	Cut off; 313(4.5)
Acetonitrile	35.94	3.54	1.60	225(3.9); 308(4.4)
MeOH	32.66	1.71	1.20	223(4.0); 309(4.45)
H_2O	78.50	1.78	0.92	226(3.9); 309(4.3)

a Relative solvent dielectric constant.

b Dipole moment in Debyes (1 D = 3.34×10^{-30} C m).

c Ratio of fluorescence intensities read at 357 nm (LE) and 377 nm (ICT) in 80% (v/v) solvent–water solutions.

d Maximum wavelength absorption (log extinction coefficient in M^{-1} cm^{-1}).

Table 2 Concentration and mixed dissociation constants of TCA determined by potentiometry and spectrophotometric titrations at 25°C.

Method	**Potentiometry**	**Spectrophotometry**
pK_1^H	2.241 ± 0.005[a]	2.27 ± 0.02[b], Ref. (*26*)
pK_2^H	8.390 ± 0.001[a]	8.24 ± 0.28, Ref. (*27*)

a This work, *I* = 0.1 M, NaCl.

b *I* = 0.12 M, buffers, Ref. (*26*).

The fluorescence spectrum of TCA in water is strongly affected by the medium acidity showing dual fluorescence emission and the intensity is strongly enhanced with the pH of the medium. Figure 1 shows the corresponding spectra recorded in strong acid (pH < 1.5), mild

acid (pH~5), basic (pH~10) and in alkaline medium. The different investigated pH regions also reflect the appearance of three different fluorescent species of TCA showing distinct fluorescence quantum yield. As the pH regions in fluorescence are similar to those observed in the ground state, it suggests no significant changes on the pK_a value of TCA in the excited state in accordance with the Förster approximation (*26* , *28*). In addition, at pH>4 (existence of TcH^+ or Tc), dual fluorescence is observed. The emitting chromophore in TCA is the benzene ring, and emission occurs from both the lowest (π, π*) singlet state (LE) and the ICT state, which is originated from the N-lone pair of the secondary amine group (acting as the electron donor group) to π-orbitals of the benzene ring or to the carbonyl group that is characterised by a high electron accepting character. An alternative view could attribute the dual emission to a π → π* transition involving a considerable charge transfer character. The scan [2] in Figure 1 corresponds to the emission of TcH^+ species, that is, when the N atom of the secondary amine group is deprotonated. Scans [3] and [4] were obtained when the tertiary amine group is also deprotonated.

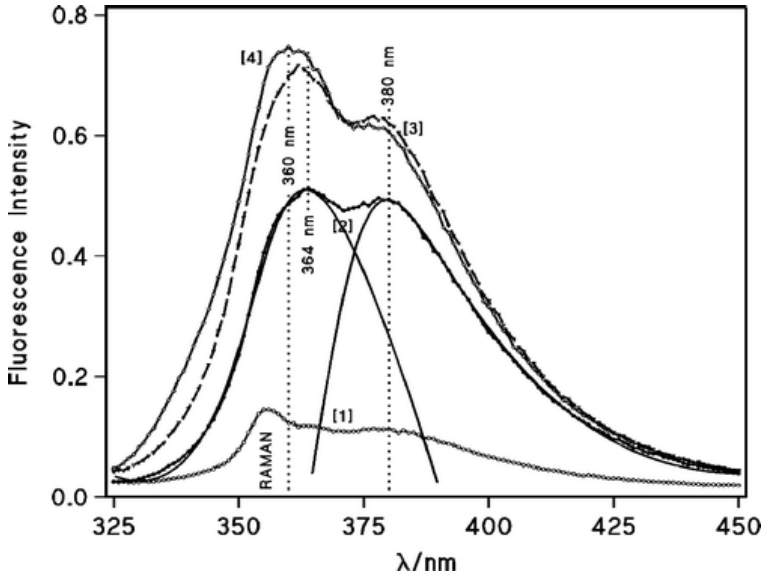

Figure 1 Emission spectra of 10.4 μM TCA in aqueous solutions of [1] hydrochloric acid 0.033 M; [2] acetic acid–acetate buffer 0.066 M pH 4.78; [3] carbonate–bicarbonate buffer 0.033 M pH 10.2, and $[OH^-]$ = 0.048 M; λ_{ex} = 315 nm.

The emission through ICT state decreases faster than the LE emission as the non-polar solvent concentration increases. Plotting the fluorescence emission intensity, I_F, for both maximum emission bands, as a function of the solvent concentration, results in Figure 2(a),(b), respectively, for emissions at 357 nm (LE) and 377 nm (ICT). Two different behaviours are clearly observed; for both dioxane and DMSO solvents, high non-linear fluorescence emission was observed whereas, in the presence of AN, good straight lines were drawn; MeOH can be seen as an intermediate situation. In the S_1 state, the polarity of the secondary amine group is further increased due to the increased charge transfer

interactions from this group to the carbonyl moiety, and the N-lone pair of the secondary amine group acts as a better proton donor. Table 1 reports the fluorescence intensity ratio of LE to ICT states measured for the same solvent concentration, along with solvent properties (*29*) and characteristics of the absorption spectra. It can be noted the decisive role of H-bonding with the solvent – the case of water and MeOH – in stabilising the optimal configuration required to observe emission from the ICT state (low ratio of I_F(LE)/I_F(ICT) determined at 10 M solvent concentration).

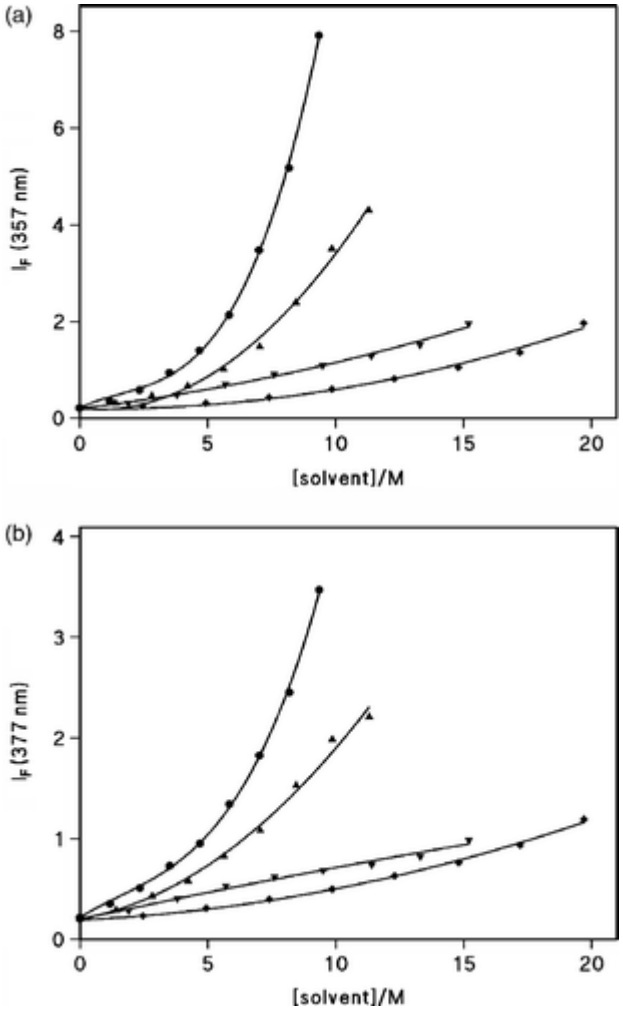

Figure 2 Plot of fluorescence intensities read at (a) 357 nm and (b) 377 nm as a function of the solvent concentration in the water–solvent mixtures; symbols correspond to dioxane (•), DMSO (▲), AN (▼) and MeOH (♦).

Another parameter that conditions the ICT state emission is the restricted motion imposed to the fluorophore. The nature of the CD microvessel constraints nuclear motions and may stabilise conformations that are less favoured in free solution. On the other hand, the hydrophobic nature of the cavity can affect photoprocesses that are sensitive to solvent polarity or dielectric properties. For this purpose, we investigated the effect of rigid hosts such as CDs in the emission of fluorescence of TCA. As mentioned elsewhere, CDs are very soluble in water but their cavity is hydrophobic. Therefore, hydrophobic species can be

‘extracted’ from water and enclosed in the CDs, with a consequent change in the luminescence properties.

Figure 3(a) shows the steady-state fluorescence spectra of TCA as a function of the acidity of the medium at constant [β-CD], whereas Figure 3(b) shows the effect of β-CD concentration on the fluorescence emission intensity recorded in aqueous solutions of 0.067 M of sodium acetate.

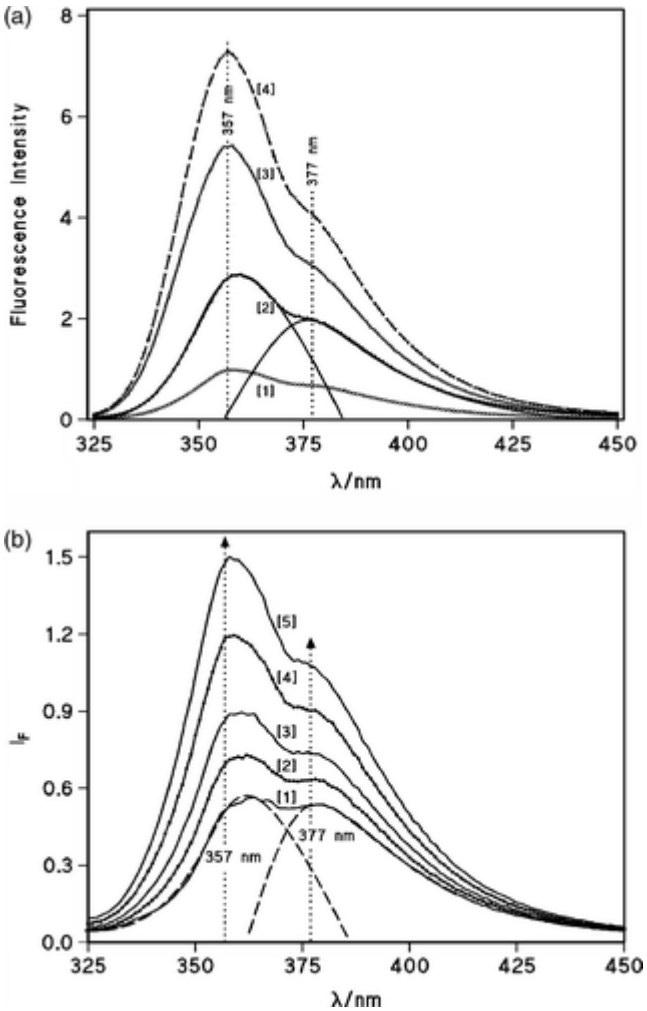

Figure 3 Emission spectra of 10.4 μM TCA in (a) aqueous β-CD (1.29 mM) solutions of [1] hydrochloric acid 0.033 M; [2] acetic acid–acetate buffer 0.066 M pH 4.78; [3] alkaline medium of $[OH^-] = 0.048$ M and [4] carbonate–bicarbonate buffer 0.033 M pH 10.2, and (b) in aqueous sodium acetate 0.067 M as a function of β-CD concentration equal to [1] 0; [2] 0.026, [3] 0.052; [4] 0.10, [5] 0.16 mM. λ_{ex} = 315 nm.

Under all experimental conditions, the addition of β-CD at increasing concentrations (up to 9 mM) induces normal spectral variations characterised by a progressive blue shift of the maximum to *c*.357 nm and large enhancement of emission intensity with respect to water (compare Figures 1 and 3(a)). In addition, the emission through the LE state is favoured over that of the ICT state – the band at 357 nm increases with both the β-CD concentration (Figure 3(b)) and the stability of the complex. The former statement is, in fact, the consequence of the latter, since as more CD is present in the medium, the quantity of the TCA forming complexes increases in accordance with Equation (1) for the case of a 1:1 stoichiometry of the inclusion complexes.

$$TCA + CD \overset{K_i^c}{\rightleftharpoons} TCA{\cdot}CD. \qquad (1)$$

In this sense, the fluorescence emission intensities, read under different experimental conditions and plotted in Figure 4, increase with β-CD concentration and level off at high CD concentration. This behaviour is indicative of inclusion complex formation of a 1:1 stoichiometry. It can also be seen, the strong effect of pH on the stability of the complex: the highest stable complex is observed in carbonate–bicarbonate buffer at very low CD concentration.

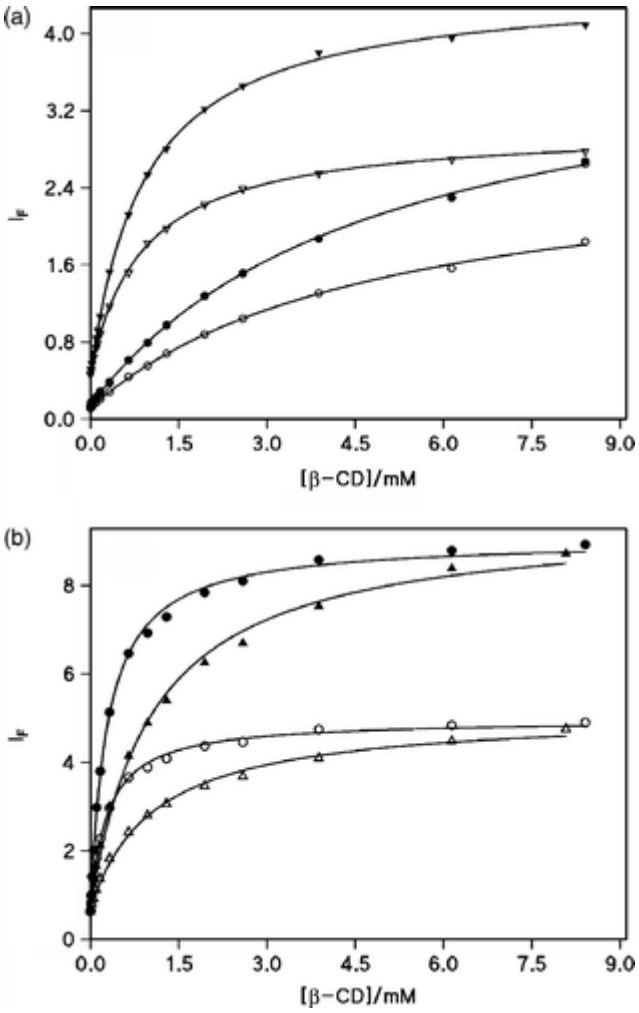

Figure 4 Variation of the fluorescence emission intensities of 10.4 μM TCA dissolved in (a) aqueous HCl 0.033 M (○,•), and in aqueous 0.067 M acetic acid–acetate (1:1) (▾, ▽) and (b) aqueous 0.048 M of NaOH (▴,Δ), and in aqueous 0.033 M carbonate–bicarbonate (1:1) buffer (○,•), as a function of β-CD concentration: (open) symbols correspond to 377 nm or ICT emission state and (solid) symbols correspond to 357 nm or LE emission state.

To understand the concept of stability of inclusion complexes, one needs to know which TCA species is included into the CD cavity. Then, by considering the acid–base equilibrium of TCA stated in Scheme 1, and that of CD, which includes the ionisation of a secondary HO group in alkaline medium (the pK_a is 12.2) (*30*), four possible different complexes of a 1:1 stoichiometry can be postulated that, a priori, could be TcH_2^{+2}·CD, TcH^+·CD, Tc·CD or $Tc{\cdot}CD^-$, i.e. neutral CD complexed with dication, monocation and neutral forms of TCA and ionised CD complexed with neutral TCA. The presence of two acid–base equilibria in a TCA

molecule, along with the own acid–base equilibrium in CD, and four possible complexation equilibrium processes make the CD–TCA system a very complex one. Nevertheless, the system results are notably simplified when the experiments are performed under determined working conditions; in addition, the main driving forces for complex formation are the hydrophobic effect that consider the exclusion of the hydrophobic guest from the bulk water solvent when intermolecular interactions are not favourable, accompanied by the release of high-energy water molecules from the CD cavity. This fact explains why the double protonated TCA molecule (TcH_2^{+2}) does not form inclusion complexes; nevertheless, even in strong acid medium, one observes spectral variations over the whole CD concentration range. Scheme 2 accounts for the experimental facts in which the TcH^+species undergoes complexation with CD by the equilibrium process of constant K_1^c or K_2^c expressed by Equations (2) and (3), respectively. The 'extraction' of TcH^+ species from water and enclosed into de CD cavity shifts the acid–base equilibrium, K_1^H, towards the basic form of TCA, i.e. TCA is a weaker base in the presence of CD.

$$K_1^c = \frac{[TcH{\cdot}CD^+][H^+]}{[TcH_2^{+2}][CD]}, \qquad (2)$$

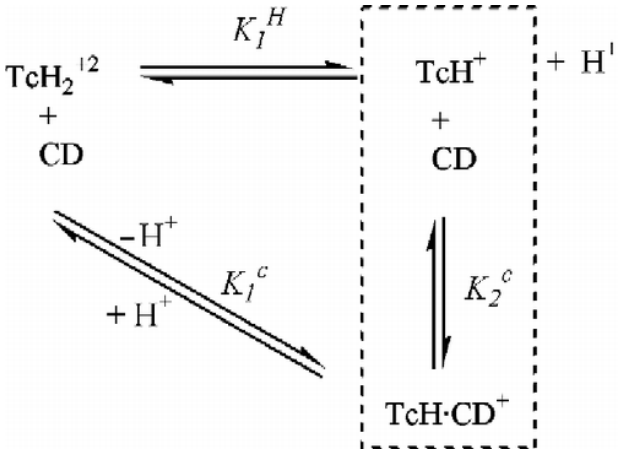

Scheme 2 Postulated equilibrium steps in TCA–CD system in strong acid medium.

$$K_2^c = \frac{[TcH{\cdot}CD^+]}{[TcH^+][CD]}. \qquad (3)$$

Under the experimental conditions of the work, i.e. $[TCA]_t \ll [CD]$, we must first consider that, in strong acid, HCl, the stoichiometric TCA concentration is given by $[TCA]_o = [TcH_2^{+2}] + [TcH^+] + [TcH \cdot CD^+]$. Second, taking into account that the quantum emission yield of TcH_2^{+2} species (TCA dication) is negligible, the measured fluorescence intensity is due to both the protonated TCA in the bulk water phase (TcH^+) and included into the CD cavity ($TcH \cdot CD^+$). Taking into account the different quantum yield (Φ) for free and included species, the total fluorescence emission is given by $I_F = \epsilon_w \ell I_o \Phi_w [TcH^+]_w + \epsilon_c \ell I_o \Phi_c [TcH \cdot CD^+]$, where ϵ is the molar absorption coefficient, ℓ = 1 cm is the path light and I_o is the absorbed intensity. This equation can be converted into Equation (4) by considering together Equations (2) and (3). In this equation, I_F^w and I_F^c represent the fluorescence intensities corresponding to the TCA free and complexed with CD, respectively, and $K_1^c = K_2^c K_1^H$.

$$I_F = \frac{I_F^w f(H^+) + I_F^c K_2^c f(H^+)[CD]}{1 + K_2^c f(H^+)[CD]} \qquad (4)$$

$$\text{with } f(H^+) = \frac{K_1^H}{K_1^H + [H^+]}.$$

Solid curves corresponding to the below two set points displayed in Figure 4(a) were drawn in the fit of Equation (4) to the experimental data read at both 357 (filled) and 377 (open) symbols. The non-linear regression analysis of this equation to the experimental data yields the values for the optimised parameters, I_F^c and K_2^c, listed in Table 3, first arrow.

In mild acid medium, i.e. in aqueous buffered solutions of acetic acid–acetate of pH>4, as the pK_1^H has been measured equal to 2.27, $[H^+] \ll K_1^H$ and Equation (4) simplifies to Equation (5). Solid curves for the above two set points in Figure 4(a) correspond to the fit of Equation (5) to the experimental data read also at both 357 (filled) and 377 (open) symbols, when the optimised parameters take the values reported in Table 3.

Table 3 Experimental conditions and optimised parameters obtained in the fitting process of Equation (4) or (5) to the experimental data, which result in the study of the influence of β-CD concentration on the steady-state fluorescence emission of TCA.

		λ = 357 nm, LE emission state			λ = 377 nm, ICT emission state		
Medium	**TCA (μM)**	I_F^w	I_F^c	K_1^c **(M^{-1})**	I_F^w	I_F^c	K_1^c **(M^{-1})**
HCl 0.035 M	10.4	0.706[a]	4.08 ± 0.06	1174 ± 16[a]	0.708[a]	2.80 ± 0.05	1178 ± 50[a]
HAc/Ac^- (1:1) 0.048 M[b]	3.6	0.258	2.09 ± 0.02	922 ± 45[c]	0.212	1.37 ± 0.01	924 ± 47[c]
HAc/Ac^- (1:1) 0.167 M[b]	3.6	0.255	2.04 ± 0.02	991 ± 50[c]	0.225	1.34 ± 0.02	989 ± 50[c]
HAc/Ac^- (1:1) 0.067 M[b]	10.4	0.451	4.50 ± 0.02	1090 ± 20[c]	0.490	3.03 ± 0.01	1113 ± 18[c]
NaAc 0.067 M[b]	10.4	0.563	5.26 ± 0.04	1412 ± 40[c]	0.535	3.40 ± 0.03	1380 ± 43[c]
HCO_3^-/CO_3^{-2} (1:1) 0.025 M[d]	3.6	0.359	3.86 ± 0.03	3344 ± 120[e]	0.283	2.10 ± 0.02	3418 ± 160[e]
HCO_3^-/CO_3^{-2} (1:1) 0.040 M[d]	3.6	0.322	3.71 ± 0.04	3354 ± 200[e]	0.249	2.12 ± 0.02	3395 ± 216[c]
HCO_3^-/CO_3^{-2} (1:1) 0.033 M[d]	10.4	0.656	9.02 ± 0.07	3464 ± 145[e]	0.63	4.96 ± 0.03	3530 ± 130[e]
NaOH 0.048 M	10.4	0.728	9.5 ± 0.2	940 ± 60[f]	0.613	5.05 ± 0.09	1010 ± 70[f]

a Equation (4) value of $f(H^+) = 0.17$.
b Buffer solutions of acetic acid (HAc)–acetate (Ac^-).
c Equation (5), K_2^c.
d Buffer solutions of carbonate–bicarbonate, pH 10.2.
e Equation (5), value of K_3^c.
f Equation (5), value of K_4^c.

$$I_F = \frac{I_F^w + I_F^c K_2^c [CD]}{1 + K_2^c [CD]}. \qquad (5)$$

In mild basic medium, i.e. in aqueous buffered solutions of carbonate–bicarbonate buffer of pH~10, the tertiary amine group of TCA is deprotonated ($pK_2^H = 8.39$). As TCA is now a neutral molecule, the hydrophobic effect is increased, since the strong ion–dipole interactions are now not possible, and one may expect a higher value for the association constant of TCA

with CD cavity. The equilibrium reaction of Equation (6), lead us to an equation of type (5) where K_2^c must be replaced by K_3^c that corresponds to the equilibrium constant of the inclusion complexes formed between both neutral forms of TCA and CD. The experimental data are displayed in Figure 4(b) and the fit to the corresponding equation (of type (5)) results in the values of the optimised parameters listed in Table 3. As expected, the value of K_3^c is nearly three-fold that of K_2^c; the difference measures the relative importance of the hydrophobic effect against the ion–dipole interactions (the energy of water release from the cavity is in both cases the same).

$$\mathrm{Tc} + \mathrm{CD} \overset{K_3^c}{\rightleftharpoons} \mathrm{Tc{\cdot}CD}. \qquad (6)$$

Finally, in alkaline medium, TCA is a neutral molecule but the host, CD, is an anion, i.e. a secondary OH group is ionised (pK_a~12.2). This group is located at the main entrance of the CD cavity; therefore, when it is ionised, the hydration level is high and makes difficult the inclusion process of a hydrophobic guest. Thus, the equilibrium reaction of Equation (7) can be proposed.

$$\mathrm{Tc} + \mathrm{CD}^- \overset{K_4^c}{\rightleftharpoons} \mathrm{Tc{\cdot}CD}^-. \qquad (7)$$

Taking into account that the TCA concentration is much lower than that of CD and proceeding as in the previous cases, we can easily arrive at an equation of type (5) to relate the changes in fluorescence emission intensity to the CD concentration in alkaline medium, where K_2^c must be replaced by K_4^c that corresponds to the stability constant of the inclusion complexes formed between the neutral form of TCA and the ionised CD, CD^-. The experimental data are also displayed in Figure 4(b) and the fit to the corresponding equation (of type (5)) results in the values of the optimised parameters listed in Table 3. These data indicate that $K_3^c > K_2^c \sim K_4^c$; the K_i^c values measured in the presence of sodium acetate are, in fact, a combined result of both K_2^c and K_3^c, because under these conditions of $\mathrm{p\tilde{H}} \sim \mathrm{p}K_2^{\mathrm{H}}$, TCA exists as both TcH^+ and Tc. In the same sense, at $[OH^-] = 0.048$ M, where the percentage of ionised β-CD is not higher than 80%, the value of $K_i^c = 1010\,\mathrm{M}^{-1}$ must be a mixed value of true K_3^c and K_4^c, i.e. the true K_4^c should be lower.

In summary, the preceding mechanistic treatment implies that the variation of I_F as a function of [CD] should follow Equation (4) or (5) depending on the experimental conditions of the experiments, where K_2^c, K_3^c and K_4^c are the stability equilibrium constants of the inclusion complexes formed between protonated tetracaine and CD ($TcH{\cdot}CD^+$), neutral tetracaine and CD (Tc·CD), and neutral tetracaine and ionised CD ($Tc{\cdot}CD^-$), respectively,

and I_F^w and I_F^c refer to the fluorescence intensity readings obtained, under each experimental condition, in water and at a CD concentration corresponding to the complete guest inclusion, respectively.

In order to study the effect of the size of the CD cavity, we analysed the effect of both α- and γ-CD. Figure 5 shows the variation of the fluorescence emission intensity as a function of the CD concentration. In every case, the plot of I_F against [CD] describes saturation curves due to the inclusion complex formation of a 1:1 stoichiometry. The nonlinear regression analysis of the experimental data to Equation (5) – valid for experiments performed in either mild acid or mild basic medium – affords the values for the optimised parameters listed in Table 4, along with the results obtained in the presence of β-CD for the sake of comparison. It can be concluded that β-CD cavity combines optimal geometry and polarity conditions with complex TCA molecules, whereas γ-CD yields the less stable complex. It is worthy to mention the restricted motion imposed by the narrow α-CD cavity, in which case the I_F^c due to LE emission is more than three-fold the value measured in the γ-CD cavity, where both the polarity (dielectric constant equal to 70 against 47 for α-CD) (*30*) and rotation freedom are high.

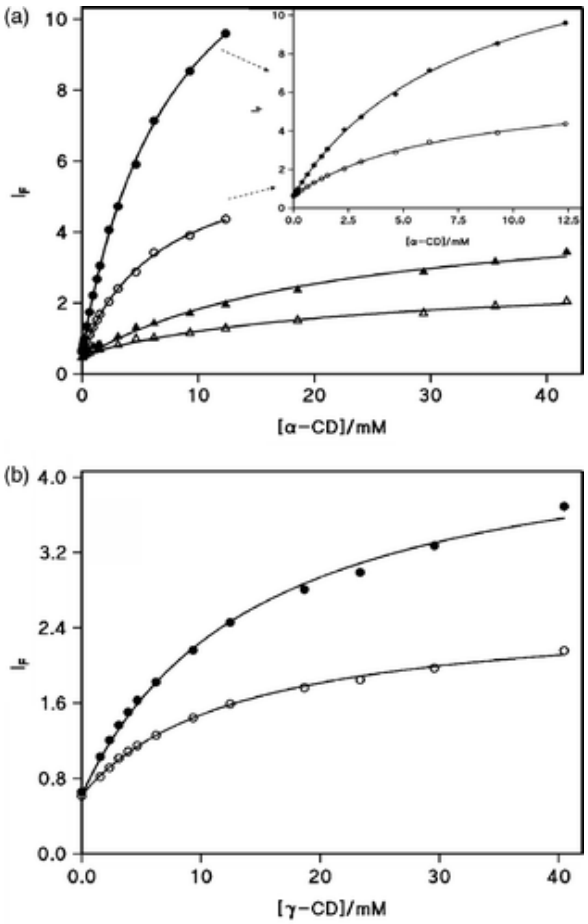

Figure 5 Variation of the fluorescence emission intensities of 10.4 μM TCA dissolved in water (a) at 0.033 M carbonate–bicarbonate (1:1) buffer (○,•) and at 0.067 M acetic acid–acetate (1:1) as a function of α-CD concentration (▾,▽); the inset shows the indicated expanded plot, and (b) at 0.033 M carbonate–bicarbonate (1:1) buffer (○,•), as a function of γ-CD concentration; (open) symbols correspond to 377 nm or ICT emission state, (solid) symbols correspond to 357 nm or LE emission state.

Table 4 Experimental conditions and parameters obtained in this study of the influence of CDs on the fluorescence emission of 10.4 μM TCA aqueous solutions.

		λ = 357 nm, LE emission state			λ = 377 nm, ICT emission state		
Medium	**Cyclodextrin**	I_F^w	I_F^c	K_3^c **(M^{-1})**	I_F^w	I_F^c	K_3^c **(M^{-1})**
HAc/Ac^- (1:1) 0.067 M[a]	α-CD	0.451	4.80 ± 0.20	46 ± 4[b]	0.495	2.7 ± 0.1	49 ± 6[b]
HCO_3^-/CO_3^{-2} buffer (1:1) 0.033 M	α-CD	0.65	15.35 ± 0.22	125 ± 4	0.61	6.5 ± 0.1	141.5 ± 5.0
HCO_3^-/CO_3^{-2} buffer (1:1) 0.033 M	β-CD	0.656	9.02 ± 0.07	3464 ± 145	0.63	4.96 ± 0.03	3530 ± 130
HCO_3^-/CO_3^{-2} buffer (1:1) 0.033 M	γ-CD	0.65	4.7 ± 0.1	65 ± 4	0.62	2.60 ± 0.04	76 ± 5

a Buffer solutions of acetic acid–acetate.

b Equation (5), value of K_2^c.

The experimental data were also fitted to the linearised form of Equation (4) or (5), i.e. the Benesi–Hildebrand relation used for these types of complexation processes and expressed in terms of fluorescence intensity with the assumption that [CD]≫[TCA·CD], i.e. the reciprocal plot of ($I_F - I_F^w$) against 1/[CD]. In every case, perfect straight lines were obtained (plots not shown) rendering similar values of K_i^c and I_F^c to those obtained from the nonlinear regression analysis.

Discussion

The UV–vis spectra of TCA indicate no significant changes in the pK_a of the ground state with respect to that of the excited state. Excitation at the lowest energy absorption band (λ_{max}~300 nm) yields dual fluorescence, where emission intensity increases drastically with both the pH and the apolar character of the medium, represented here by aqueous solvent mixtures or aqueous CD solutions. TCA forms 1:1 inclusion complexes with α-, β- or γ-CD; only the protonated (at the tertiary amine group) or neutral TCA molecules are able to be included into the CD cavity; however, the highest complex stability was obtained in conditions of neutral host and guest, i.e. at pH~10 in bicarbonate–carbonate buffered solutions. The size of the CD cavity affects both the complex stability and dual fluorescence emission.

In aqueous solvent mixtures up to 80% (v/v) solvent–water, TCA shows dual nonlinear fluorescence, except for the case of AN, in which medium nearly straight lines of I_F vs. [solvent] was obtained. By contrast, in aqueous CD solutions, the I_F vs. [CD] increases at low CD concentrations and levels off at high concentration of the host, when almost all TCA molecules are forming complexes.

In aqueous buffered solutions of acetic acid–acetate, or even in aqueous sodium acetate solutions, the quotient between the fluorescence intensities of LE (~357 nm) and of ICT (~377 nm) is nearly 1, scan 2 in Figure 1, i.e. the ICT emission state is as important as the LE emission. This fact is contrary to the behaviour observed in those fluorophores bearing a dialkylamine group bonded in the *p*-position of the phenyl ring to the acceptor group like, for instance, methyl *p*-dimethylamine benzoate, *p*-(*N*,*N*-dimethyl-amine) benzoic acid (*22*), which in pure water emits only LE fluorescence at short wavelength. We could attribute this difference to the ability of TCA to form H-bonding with water through the secondary amine group, a fact that would enhance the stability of ICT. In this sense, the ratio of I_{LE}/I_{ICT} increases proportional to the solvent concentration in the aqueous mixtures, showing the greatest effect in aqueous dioxane mixtures (Figure 6(a)), i.e. in the less polar and aprotic solvent (see Table 2 for solvent properties), where the ICT state is not stabilised and TCA emits nearly LE fluorescence.

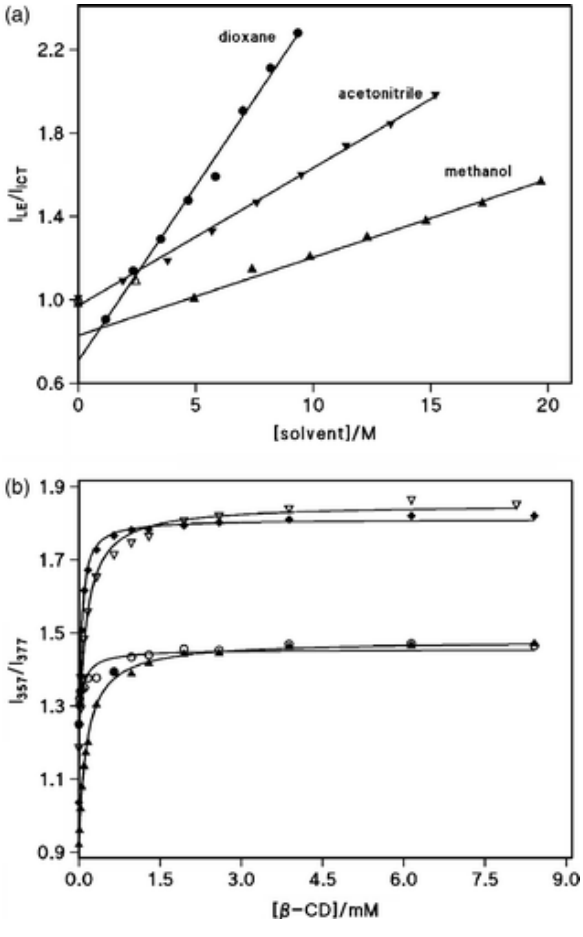

Figure 6 Plot of the ratio I_{LE}/I_{ICT} as a function of (a) solvent concentration in the aqueous mixture dioxane (•), AN (▾), MeOH (▴); (b) β-CD concentration in strong acid, HCl (▴); mild acid, acetic acid–acetate (○); mild base, carbonate–bicarbonate (▽), and alkaline medium (♦).

In aqueous CD solutions, the plot of I_{LE}/I_{ICT} against [CD] increases also with [CD], but drawing saturation curves that level off at high CD; in addition, the I_{LE}/I_{ICT} vs. [CD] profiles show similar shape for α-, β- or γ-CD. Figure 6(b) shows representative data for the case of β-CD. Again, this behaviour is contrary to that observed with, for example, DEABA in which case, first, the ICT emission intensity is higher than the LE emission (i.e. I_{ICT}/I_{LE} increases with [β-CD]) and, second, the observed behaviour in β-CD is opposite to that seen with α-CD (*22* , *23*).

Our results indicate that the CD cavity provides a less polar and aprotic environment that favours LE emission over the ICT state, because of the destabilisation of the latter due to the absence of H-bonding interactions and the constricted confinement that difficult rotation to achieve the optimal orthogonal position between donor and acceptor groups. The saturation value observed in I_{LE}/I_{ICT} vs. [CD] plots depends on the nature of TCA molecule forming complexes. In α-CD, the maximum value of I_{LE}/I_{ICT}~1.5 at pH < 5 increases to 2.1 at pH>10; in β-CD, the maximum values of this quotient increase from 1.4 at pH < 5 to approximately 1.8 at pH>10 (see Figure 6(b)), whereas with γ-CD the value of I_{LE}/I_{ICT} obtained at high CD concentration is ~1.6 even at pH~10. These facts suggest the existence of different inclusion complexes. With α- and β-CD, we can propose two possible conformations for the inclusion complex; in both, the unprotonated secondary amine group first enters into the CD cavity, but the protruding depth is higher when TCA is neutral (high hydrophobic effect that 'push' the TCA molecules out of the bulk water phase), and perhaps the secondary HO groups of the main entrance of CD are H-bonded to the carbonyl group of TCA; when TCA is a single positively charged molecule, the ion–dipole interactions with water 'pulls' them out of the cavity. Geometrical optimisation of the TCA structure with the AM1 program yields the form and dimensions of TCA displayed in Scheme3 and compared to that of CD.

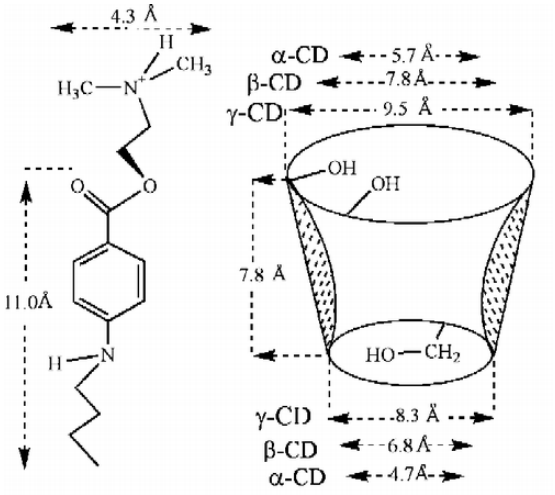

Scheme 3 Sizes of minimised energy structure of TCA compared to CDs.

Conclusions

TCA shows dual fluorescence in either water–solvent mixtures or aqueous CD solutions. The ratio of normal emission intensity to the ICT emission increases with CD concentration and levels off at high concentrations, whereas, in water–solvent mixtures, straight lines were observed. The behaviour is different from the most studied fluorophores of type dimethylamino benzonitrile. On the other hand, the stability of inclusion complex formed between TCA and CDs depends on the pH of the medium and on the CD nature; the most stable complex was observed with β-CD in mild basic medium of pH∼10. While, with α- and β-CD, the results suggest the existence of two different inclusion complexes, with γ-CD, one conformation for the inclusion complex suffices to explain the experimental observations.

Acknowledgements

Financial support from the Dirección General de Investigación (Ministerio de Educación y Ciencia) of Spain and FEDER (Project CTQ2005-07428/BQU) and from Dirección General de Programas y Transferencia de Conocimiento (Ministerio de Ciencia e Innovación) of Spain (Project CTQ2008-04429/BQU) is gratefully acknowledged. I. Iglesias-García also thanks the Ministerio de Educación y Cicncia of Spain for a research training grant.

References

1. Ragsdale, D.S., McPhee, J.C., Schener, T. and Catterall, W.A. 1994. *Science*, 265: 1724–1727.

2. (a) Vanderkooi, G.; Adade, A.B. Biochemistry **1986**, 25, 7118–7124. (b) Neeraj, A.; Vijay, K.K. Biochim. Biophys. Acta**1984**, 764, 316–323. (c) Yokoyama, S. Toxicol. Lett. **1998**, 100–101, 365–368

3. (a) Mertz, C.J.; Marques, A.D.S.; Williamson, L.N.; Lin, C.T. Photochem. Photobiol. **1990**, 51, 427–437. (b) García-Soto, J.; Fernández, M.S.; Biochim. Biophys. Acta Biomembranes **1983**, 731, 275–281. (c) Fernández, M.S.; Calderón, E. J. Photochem. Photobiol. B **1990**, 7, 75–86

4. Szejtli, J. 1988. *Cyclodextrin Technology. Topics in Inclusion Science*, Dordrecht: Kluwer.

5. Jicsinszky, L., Fenyvesi, É., Hashimoto, H. and Ueno, A. 1996. *Comprehensive Supramolecular Chemistry*, Edited by: Szejtli, J. and Osa, T. 5–40. Oxford: Pergamon. Vol. 3, Chapter 2

6. Kim, Y.H., Cho, D.W., Yoon, M. and Kim, D. 1996. *J. Phys. Chem.*, 100: 15670–15676.

7. Monti, S., Flamigni, L., Martelli, A. and Bortolus, P. 1998. *J. Phys. Chem.*, 92: 4447–4451.

8. Tee, O.S. Carbohydr. Res. **1989**, 192, 181–195; Tee, O.S. Adv. Phys. Org. Chem. **1994**, 29, 1–85; Tee, O.S.; Bozzi, M; Hoeven, J.J.; Gadosy, T.A. J. Am. Chem. Soc. **1993**, 115, 8990–8998

9. Iglesias, E. J. Am. Chem. Soc. **1998**, 120, 13057–13069; Iglesias, E. J. Org. Chem. **2003**, 68, 2689–2697

10. Grabowski, Z.R.; Rotkiewiez, K.; Siemiarezuk, A.; Cowley, D.J.; Baumann, W. Nouv. J. Chim. **1979**, 3, 443–454; Grabowski, Z.R. Pure Appl. Chem. **1993**, 65, 1751–1756

11. Lippert, E.; Lüeder, W.; Moll, F.; Näegele, W.; Böos, H.; Prigge, H.; Seibold-Blankenstein, I. Angw. Chem. **1961**, 73, 695–706; Lippert, E.; Rettig, W.; Bonacic-Koutecký, V.; Heisel, F.; Miehé, J. Adv. Chem. Phys. **1987**, 68, 1–173

12. Grawbowki, Z.R., Rotkiewicz, K. and Rettig, W. 2003. *Chem. Rew.*, 103: 3899–4031. and references therein

13. Monti, S.: Marconi, G.; Manoli, F.; Bortolus, P.; Mayer, B.; Grabner, G.; Köhler, B.; Boszczyk, W.; Rotkiewicz, K. Phys. Chem. Chem. Phys. **2003**, 5, 1019–1026; Monti, S.; Bortolus, P.; Manoli, F.; Marconi, G.; Grabner, G.; Köhler, B.; Mayer, B.; Boszczyk, W.; Rotkiewicz, K. Photochem. Photobiol. Sci. **2003**, 2, 203–211

14. Mahanta, S., Singh, R.B., Kar, S. and Guchahait, N. 2008. *J. Photochem. Photobiol. A*, 194: 318–326.

15. Abdel-Shafi, A.A. 2007. *Spectrochim. Acta A*, 66: 1228–1236.

16. Stalin, T. and Rajendiran, N. 2006. *Chem. Phys.*, 322: 311–322.

17. Krishnamoorthy, G. and Dogra, S.K. 2000. *J. Phys. Chem. A*, 104: 2542–2551.

18. Mac, M., Najbar, J. and Wirz, J. 1995. *J. Photochem. Photobiol. A*, 88: 93–104.

19. Nag, A.; Kundu, T.; Bhattacharyya, K. Chem. Phys. Lett. **1989**, 160, 257–260; Nag, A.; Bhattacharyya, K. J. Chem. Soc. Faraday Trans. **1990**, 86, 53–54

20. Al-Hassan, K.A.; Klein, U.K.A.; Suwaiyan, A. Chem. Phys. Lett. **1993**, 212, 581–587; Al-Hassan, K.A. Chem. Phys. Lett.**1994**, 227, 527–532

21. Kundu, S.; Chattopadhyay, N. J. Mol. Struct. **1995**, 344, 151–155; Kundu, S.; Chattopadhyay, N. J. Photochem. Photobiol. A**1995**, 88, 105–108

22. Jiang, Y.-B. J. Photochem. Photobiol. A **1995**, 88, 109–116; Jiang, Y.-B. Spectrochim. Acta **1995**, 51A, 275–282

23. Kim, Y.H., Cho, D.W., Yoon, M. and Kim, D. 1996. *J. Phys. Chem.*, 100: 15670–15676.

24. Rappoport, D. and Furche, F. 2004. *J. Am. Chem. Soc.*, 126: 1277–1284.

25. Iglesias, E. 2006. *J. Org. Chem.*, 71: 4383–4392.

26. Iglesias, E. 2008. *New J. Chem.*, 32: 517–524.

27. Perrin, D.D., Dempsey, B. and Serjeant, E.P. 1981. *pKa Prediction for Organic Acids and Bases*, London: Chapman and Hall.

28. Förster, T. Naturwissenschaften **1946**, 6, 166; Ireland, J.F.; Wyatt, P.A.H. In Advances in Physical Organic Chemistry: Gold, V., Bethell, D., Eds.; Academic Press: London, 1976; Vol. 12, p 132

29. Reichardt, C. 1988. *Solvent and Solvent Effects in Organic Chemistry*, 2nd ed., 408Weinheim: VCH.

30. The pK_a values determined at 25°C by potentiometry are 12.33, 12.20 and 12.08, respectively to α, β- and γ-cyclodextrin; see Comprehensive Supramolecular Chemistry, Vol. 3. Cyclodextrins, Szejtli, J.; Osa, T. Eds.; Pergamon, 1996, Chapter 1, p 17

31. Dewar, M.J.S., Zoebisch, E.G., Healy, E.F. and Stewart, J.J.P. 1985. *J. Am. Chem. Soc.*, 107: 3902 Program HyperChem 5.0, Hypercube, 1996